Non-Template-Centered, Closed Tetravanadium Phosphate and Phosphonate Clusters

Tom Otieno,[1a] Ladd M. Mokry, Marcus R. Bond,[1b] Carl J. Carrano,* and Norman S. Dean

Department of Chemistry, Southwest Texas State University, San Marcos, Texas 78666

Received August 4, 1995[⊗]

Tetranuclear V(III) complexes, $[HB(pz)_3]_4V_4(\mu\text{-}C_6H_5OPO_3)_4$ (**I**), its acetonitrile solvate (**I**·$4CH_3CN$), and $[HB(pz)_3]_4V_4(\mu\text{-}O_2NC_6H_4OPO_3)_4\cdot 4C_7H_8\cdot H_2O$ (**II**), and tetranuclear vanadyl complexes, $(t\text{-Bupz})_4V_4O_4(\mu\text{-}C_6H_5PO_3)_4\cdot 2H_2O$ (**III**) and $(t\text{-Bupz})_5V_4O_4(\mu\text{-}C_6H_5PO_3)_4\cdot 4CH_3CN\cdot 0.6\ H_2O$ (**IV**), have been prepared and characterized by spectroscopic, magnetic, and electrochemical methods (pz = pyrazole, *t*-Bupz = *tert*-butylpyrazole). The use of organic solvents and bulky organic groups as ancillary ligands leads to formation of neutral species instead of the anionic clusters commonly found in the hydrothermal synthesis of vanadium organophosphate/phosphonate systems. Complexes **I**·$4CH_3CN$ and **IV** have also been characterized by single-crystal X-ray diffraction. Crystal data: **I**·$4CH_3CN$, triclinic, $P\bar{1}$, $a = 15.495(3)$ Å, $b = 17.000(3)$ Å, $c = 17.949(4)$ Å, $\alpha = 89.17(3)°$, $\beta = 86.00(3)°$, $\gamma = 78.60(3)°$, $Z = 2$; **IV**, triclinic, $P\bar{1}$, $a = 15.541(3)$ Å, $b = 16.340(2)$ Å, $c = 19.069(5)$ Å, $\alpha = 83.58(2)°$, $\beta = 79.67(2)°$, $\gamma = 63.68(1)°$, $Z = 2$. Both are closed clusters, the core structure of the first consisting of a cubane-like arrangement of metal octahedra and phosphate tetrahedra and the core structure of the second consisting of a distorted, collapsed variant of the first. Unlike other vanadium phosphate clusters, these compounds form in the absence of a central, templating agent. As such they represent the simplest form of a closed cluster in which steric forces and cluster connectivity requirements play the primary role in organizing the cluster framework.

Introduction

Vanadium phosphate systems have garnered a significant amount of attention over recent years because of their structural diversity,[2−18] catalytic activity,[13,19] size selective sorbent properties,[13] and utility as ion exchangers.[20] Further interest in the structural diversity of these systems arises from the plethora of cagelike vanadium phosphate clusters that have been observed to form around a variety of template molecules or ions.[2,4−7,18] The potential for developing a useful set of host−guest chemistries with high specificities for guest molecules or ions based on vanadium phosphate cluster hosts continues to fuel the exploration of these systems.[21] Our motives for investigating vanadium complexes lie along different but not dissimilar lines. We have an interest in developing vanadium complexes that show specific interactions with biological phosphates, particularly DNA. In light of this we have initiated a study of the interactions between vanadium complexes and simple organic phosphates at ambient temperature and pressure. In contrast to the prevailing hydrothermal synthetic techniques, our synthetic methods more closely mimic the physical conditions present in most biological systems and have allowed us to develop a series of new vanadium phosphate clusters.[17]

We have already described in brief the initial results of this project and pointed out the wide range of nuclearity in vanadium cluster complexes that can be achieved at ambient conditions by varying the number of open coordination sites on the vanadium center and the denticity of the bridging phosphate ligand.[17] Further study of the structures of three vanadyl phosphate clusters synthesized by our group has also lead us to examine carefully the architectural components of these clusters.[18] In this vein we report here the synthesis and characterization of $[HB(pz)_3]_4V_4(\mu\text{-}C_6H_5OPO_3)_4$ (**I** and its acetonitrile solvate **I**·$4CH_3CN$), $[HB(pz)_3]_4V_4(\mu\text{-}O_2NC_6H_4OPO_3)_4\cdot 4C_7H_8\cdot H_2O$ (**II**), $(t\text{-Bupz})_4V_4O_4(\mu\text{-}C_6H_5PO_3)_4\cdot 2H_2O$ (**III**), and $(t\text{-Bupz})_5V_4O_4(\mu\text{-}C_6H_5PO_3)_4\cdot 4CH_3CN\cdot 0.6\ H_2O$ (**IV**) (pz = pyrazole, *t*-Bupz = *tert*-butylpyrazole), four tetrametallic vanadium systems that establish fundamental structures for closed poly(vanadium phosphate) clusters.

Experimental Section

Materials. Unless otherwise stated, all chemicals were reagent grade and used as such without further purification. Solvents were dried and purified using standard procedures. The disodium salts of phenyl

* Author to whom correspondence should be addressed.

⊗ Abstract published in *Advance ACS Abstracts,* January 15, 1996.

(1) (a) Present address: Department of Chemistry, Eastern Kentucky University, Richmond, KY 40475. (b) Present address: Department of Chemistry, Southeast Missouri State University, Cape Girardeau, MO 63701.
(2) Chen, Q.; Zubieta, J. *J. Chem. Soc., Chem. Commun.* **1994**, 2663.
(3) Chen, Q.; Salta, J.; Zubieta, J. *Inorg. Chem.* **1993**, *32*, 4485.
(4) Huan G.; Day, V. W.; Jacobson, A. J.; Goshorn, D. P. *J. Am. Chem. Soc.* **1991**, *113*, 3188.
(5) Salta, J.; Chen, Q.; Chang, Y.; Zubieta, J. *Angew. Chem., Int. Ed. Engl.* **1994**, *33*, 757.
(6) Müller, A.; Hovemeier, K.; Rohlfing, R. *Angew. Chem., Int. Ed. Engl.* **1992**, *31*, 1192.
(7) Huan, G.; Jacobson, A. J.; Day, V. W. *Angew. Chem., Int. Ed. Engl.* **1991**, *30*, 422.
(8) Haushalter, R. C.; Wang, Z.; Thompson, M. E.; Zubieta, J.; O'Connor, C. J. *Inorg. Chem.* **1993**, *32*, 3966.
(9) Villeneuve, G.; Suh, K. S.; Amorós, P.; Casan, N.; Beltrán, D. *Chem. Mater.* **1992**, *4*, 108.
(10) Beltrán, D.; Amorós, P.; Ibánez, R.; Martinez, E.; Beltrán, A.; Bail, A. L.; Ferey, G.; Villeneuve, G. *Solid State Ionics* **1989**, *32/33*, 57.
(11) Haushalter, R. C.; Wang, Z.; Thompson, M. E.; Zubieta, J. *Inorg. Chem.* **1993**, *32*, 3700.
(12) Soghomonian, V.; Haushalter, R. C.; Chen, Q.; Zubieta, J. *Inorg. Chem.* **1994**, *33*, 1700.
(13) Johnson, J. W.; Jacobson, A.; Butler, W. M.; Rosenthal, S. E.; Brody, J. F.; Lewandowski, J. T. *J. Am. Chem. Soc.* **1989**, *111*, 381.
(14) Huan, G.; Jacobson, A. J.; Johnson, J. W.; Corcoran, E. W., Jr. *Chem. Mater.* **1990**, *2*, 91.
(15) Kang, H. Y.; Lee, W. C.; Wang, S. L.; Lii, K. H. *Inorg. Chem.* **1992**, *31*, 4743.
(16) Lii, K.; Wu, L.; Gau, H. *Inorg. Chem.* **1993**, *32*, 4153.
(17) Mokry, L. M.; Thompson, J.; Bond, M. R.; Otieno, T.; Mohan, M.; Carrano, C. J. *Inorg. Chem.* **1994**, *33*, 2705.
(18) Bond, M. R.; Carrano, C. J.; Mokry, L. M.; Otieno, T.; Thompson, J. *Inorg. Chem.* **1995**, *34*, 1894.
(19) Centi, G.; Trifiro, F.; Ebner, J. R.; Franchetti, V. M. *Chem. Rev.* **1988**, *88*, 55.
(20) Clearfield, A. *Chem. Rev.* **1988**, *88*, 125.
(21) Reuter, H. *Angew. Chem., Int. Ed. Engl.* **1992,** *31*, 1185

0020-1669/96/1335-0850$12.00/0

phosphate and its 4-nitro analog, $C_6H_5OPO_3Na_2{\cdot}2H_2O$ and 4-$O_2NC_6H_4OPO_3Na_2{\cdot}6H_2O$, diphenyl phosphate, $(C_6H_5O)_2PO_2H$, and phenylphosphonic acid, $C_6H_5PO_3H_2$, were obtained from Aldrich. The sodium salts of the latter two were obtained as white solids via neutralization of aqueous solutions of the acids with appropriate equivalents of $NaHCO_3$, followed by evaporation of the solvent. $HB(pz)_3VCl_2DMF$,[22] (*t*-Bupz)$_2VOCl_2$,[23] and [(*t*-Bupz)$_4VO(H_2O)]Cl_2$[23] were prepared according to literature procedures.

[HB(pz)$_3$]$_4$V$_4$(μ-C$_6$H$_5$OPO$_3$)$_4$, I, and I·4CH$_3$CN. Nitrogen gas was bubbled through a mixture of 40 mL of acetonitrile and 3 mL of water for 0.5 h. The following steps were then carried out under an atmosphere of nitrogen using standard Schlenk techniques. $HB(pz)_3VCl_2DMF$ (0.40 g, 0.98 mmol) was dissolved in 30 mL of the solvent mixture with the remainder of the solvent mixture used to dissolve $C_6H_5OPO_3Na_2{\cdot}2H_2O$ (0.25 g, 0.98 mmol). The two solutions were mixed together, stirred for 2 h, and then filtered to remove sodium chloride. The filtrate was left standing for 3−4 days under a nitrogen atmosphere during which time large green crystals formed. These were shown by X-ray diffraction analysis to be $[HB(pz)_3]_4V_4(\mu\text{-}C_6H_5OPO_3)_4{\cdot}4CH_3CN$, **I**·4CH$_3$CN. The crystals readily lose solvent on drying under vacuum to give compound **I**. Yield of **I**: 0.18 g (43%). Anal. Calcd for $C_{60}H_{60}N_{24}O_{16}P_4B_4V_4$: C, 41.32; H, 3.47; N, 19.27. Found: C, 41.19; H, 3.54; N, 19.33. UV−vis, λ_{max} (ϵ, L mol^{-1} cm^{-1}): 410 (shoulder), 604 (63) (nm). IR (cm^{-1}): ν_{B-H} = 2479 (m), ν_{P-O} = 1225 (s), 1214 (s), 1176 (s), 1051 (s).

[HB(pz)$_3$]$_4$V$_4$(μ-4-O$_2$NC$_6$H$_4$OPO$_3$)$_4$·4C$_7$H$_8$·H$_2$O, II. This compound was prepared following the same procedure as above using 0.20 g (0.49 mmol) of $HB(pz)_3VCl_2DMF$ and 0.18 g (0.48 mmol) of 4-$O_2NC_6H_4OPO_3Na_2{\cdot}6H_2O$. The green solid product obtained was recrystallized from hot toluene. X-ray crystallography established the chemical formula of the compound as $[HB(pz)_3]_4V_4(\mu\text{-}4\text{-}O_2NC_6H_4OPO_3)_4{\cdot}4C_7H_8{\cdot}H_2O$, but elemental analysis indicates partial loss of solvent on drying. Yield: 0.12 g (46%). Anal. Cacld for $C_{74}H_{74}N_{28}O_{25}P_4B_4V_4$: C, 41.80; H, 3.51; N, 18.44. Found: C, 41.78; H, 3.62; N, 18.38. UV−vis, λ_{max} (ϵ, L mol^{-1} cm^{-1}): 430 (shoulder), 593 (58) nm. IR (cm^{-1}): ν_{B-H} = 2488 (m), ν_{P-O} = 1226 (s), 1213 (s), 1180 (s), 1052 (s).

(*t*-Bupz)$_4$V$_4$O$_4$(μ-C$_6$H$_5$PO$_3$)$_4$·2H$_2$O, III. To (*t*-Bupz)$_2VOCl_2$ (0.80 g, 2.07 mmol) was added 40 mL of water, and the mixture was stirred for several minutes, briefly heated in a steam bath, and then filtered. To the blue filtrate was added 0.42 g (~2 mmol) of $C_6H_5PO_3Na_2{\cdot}xH_2O$. The blue precipitate obtained was collected, dried, and recrystallized from ethanol. Yield: 0.32 g (43%). Anal. Calcd for $C_{52}H_{72}N_8O_{18}P_4V_4$: C, 43.83; H, 5.09; N, 7.86. Found: C, 44.01; H, 5.49; N, 7.83. UV−vis, λ_{max} (ϵ, L mol^{-1} cm^{-1}): 380 (431), 510 (99), 640 (94), 802 (147) nm. IR (cm^{-1}): ν_{V-O} = 957 (s), ν_{P-O} = 1164 (s), 1138 (s), 1111 (s), 1036 (s), 1019 (s), 996 (s). The anhydrous complex, which readily picks up water again if exposed to the atmosphere, may be obtained by drying the dihydrate at 100 °C under vacuum. Anal. Calcd for $C_{52}H_{68}N_8O_{16}P_4V_4$: C, 44.97; H, 4.94; N, 8.06. Found: C, 44.66; H, 5.02; N, 7.96. Identical products are obtained if [(*t*-Bupz)$_4$VO(H$_2$O)]Cl$_2$ is used as the source of vanadium(IV).

(*t*-Bupz)$_5$V$_4$O$_4$(μ-C$_6$H$_5$PO$_3$)$_4$·4CH$_3$CN·0.6 H$_2$O, IV. Recrystallization of the precipitate obtained in the preparation of **III** from acetonitrile, rather than from ethanol, gave a mixture of blue and purple solids. Attempts at bulk separation of these two compounds by washing with different solvents were unsuccessful. However a suitable crystal for X-ray structural analysis of the blue product was obtained by physical separation from the mixture. The X-ray analysis showed the compound to be (*t*-Bupz)$_5V_4O_4(\mu\text{-}C_6H_5PO_3)_4{\cdot}4CH_3CN{\cdot}0.6\ H_2O$. Both the blue and purple solids are soluble in methylene chloride, with the former having a slightly lower solubility. Hence, we were able to obtain a very small clean sample of the blue solid for elemental analysis by washing the mixture with methylene chloride. The sample readily loses its crystallinity on washing with methylene chloride, indicating loss of solvate molecules from the lattice. Anal. Calcd for $C_{59}H_{80}N_{10}O_{16}P_4V_4$: C, 46.84; H, 5.33; N, 9.26. Found: C, 46.58; H, 5.21; N, 9.30. Unfortunately neither of the two products could be separated in pure form in sufficient quantities for further characterization.

Table 1. Crystallographic Data for $[HB(pz)_3]_4V_4(\mu\text{-}C_6H_5OPO_3)_4{\cdot}4CH_3CN$, **I**·4CH$_3$CN, and (*t*-Bupz)$_5V_4O_4(\mu\text{-}C_6H_5PO_3)_4{\cdot}4CH_3CN{\cdot}0.6\ H_2O$, **IV**[a,b]

compound	**I**·4CH$_3$CN	**IV**
formula	$C_{68}H_{72}N_{28}O_{16}B_4P_4V_4$	$C_{67}H_{92}N_{14}O_{16.6}P_4V_4$
fw	1908.4	1686.8
space group	$P\bar{1}$	$P\bar{1}$
a, Å	15.495(3)	15.541(3)
b, Å	17.000(3)	16.340(2)
c, Å	17.949(4)	19.069(5)
α, deg	89.17(3)	83.58(2)
β, deg	86.00(3)	79.67(2)
γ, deg	78.60(3)	63.68(1)
V, Å^3	4623.5(16)	4267(2)
Z	2	2
ρ_{calcd}, g cm^{-3}	1.371	1.313
μ, cm^{-1}	5.35	5.66
T, °C	25	25
radiation (λ, Å)	Mo Kα (0.71073)	Mo Kα (0.71073)
R	0.0478	0.0794
w*R*	0.0655	0.0789

[a] Estimated standard deviations in the least significant digit are given in parentheses. [b] Quantity minimized = $\sum w(F_o - F_c)^2$, $w = [\sigma^2(F) + (0.0008)F^2]^{-1}$, $R = \sum||F_o| - |F_c||/\sum F_o$, and $R_w = (\sum(w[F_o - F_c]^2/\sum(wF_o^2))^{1/2}$.

Physical Measurements. Elemental analyses were performed by Desert Analytics, Tucson, AZ. Infrared spectra were obtained on a Perkin-Elmer 1600 FT-IR spectrometer as KBr pellets. UV−vis spectra of samples dissolved in dichloromethane were recorded on an HP 8520 diode array spectrophotometer. EPR spectra were recorded on a MicroNow 8300A X-band spectrometer. Quartz flat cells were used for high dielectric solvents, and cylindrical quartz tubes were employed for low dielectric solvents. Cyclic voltammetry on Pt bead electrodes was performed as previously described using a BAS CV-27 electrochemical analyzer.[24] Dry methylene chloride (Burdick and Jackson "Distilled in Glass" grade) was used as the solvent with 0.1 M tetrabutylammonium hexafluorophosphate as a supporting electrolyte. Potentials were measured vs a Ag/AgCl reference electrode with the ferrocene/ferrocinium couple used as an internal standard. Variable temperature magnetic susceptibilities for **I**·4CH$_3$CN were measured in the temperature range 5−280 K on an LDJ 9600 vibrating sample magnetometer using procedures described previously.[18] The magnetic data were corrected for the diamagnetism of the constituent atoms using Pascal's constants.[25]

X-ray Data Collection and Analysis. Crystals of **I**·4CH$_3$CN, **II**, and **IV** were sealed in Lindemann glass capillaries and mounted on a Siemens P4 diffractometer. Inclusion of a small amount of mother liquor in the capillary was necessary in order to preserve the crystallinity of **IV** during the data collection. Unit cell constants were determined by least-squares refinement of the angular settings of 12−30 well-centered, high-angle reflections. Structure solution and refinement were achieved by means of the SHELXTL-PLUS software package provided by Siemens.[26] Structures were solved by direct methods (**I**·4CH$_3$CN and **II**) and by the Patterson technique (**IV**). Hydrogen atom positions were calculated to give an idealized geometry and constrained to ride on their bound atoms. Anisotropic thermal parameters were refined for fully undisordered non-hydrogen atoms. Crystallographic data for **I**·4CH$_3$CN and **IV** are reported in Table 1. Atomic positions and equivalent isotropic thermal parameters for the cluster atoms are reported in Table 2 for **I**·4CH$_3$CN and Table 3 for **IV**. Additional details of each refinement are discussed below.

The presence of markedly elongated thermal ellipsoids on three atoms of the phenyl ring pendant to P(3) in the structure of compound **I**·

(22) Mohan, M.; Holmes, S. M.; Butcher, R. J.; Jasinski, J. P.; Carrano, C. J. *Inorg. Chem.* **1992**, *31*, 2029.
(23) Mohan, M.; Bond, M. R.; Otieno, T.; Carrano, C. J. *Inorg. Chem.* **1995**, *34*, 1233.
(24) Bonadies, J. A.; Carrano, C. J. *J. Am. Chem. Soc.* **1986**, *108*, 4088.
(25) O'Connor, C. J. *Prog. Inorg. Chem.* **1982**, *203*, 29.
(26) Sheldrick, G. M. *SHELXTL-PC, Version 4.1;* Siemens X-ray Analytical Instruments, Inc.: Madison, WI, 1989. Scattering factors from *International Tables for X-ray Crystallography*; Ibers, J., Hamilton, W., Eds.; Kynoch: Birmingham, England, 1974; Vol. IV.

Table 2. Atomic Coordinates ($\times 10^4$) and Equivalent Isotropic Displacement Coefficients ($Å^2 \times 10^3$) for $[HB(pz)_3]_4V_4(\mu\text{-}C_6H_5OPO_3)_4\cdot 4CH_3CN$[a]

	x	*y*	*z*	U_{eq}[b]
V(1)	5323(1)	7189(1)	1116(1)	34(1)
V(2)	7569(1)	8839(1)	1767(1)	37(1)
V(3)	8016(1)	5914(1)	2455(1)	38(1)
V(4)	5564(1)	7919(1)	3803(1)	32(1)
P(1)	5428(1)	8773(1)	2166(1)	31(1)
P(2)	7512(1)	7066(1)	1017(1)	36(1)
P(3)	7727(1)	7696(1)	3238(1)	35(1)
P(4)	5800(1)	6330(1)	2711(1)	33(1)
O(1)	5576(2)	6379(2)	1905(2)	39(1)
O(2)	6855(2)	7633(2)	3610(2)	42(1)
O(3)	6554(2)	7260(2)	864(2)	43(1)
O(4)	6766(2)	6080(2)	2819(2)	42(1)
O(5)	7839(2)	7745(2)	1354(2)	41(1)
O(6)	4765(2)	9588(2)	1951(2)	43(1)
O(7)	6291(2)	8917(2)	1825(2)	49(1)
O(8)	7720(2)	8464(2)	2795(2)	43(1)
O(9)	7790(2)	6286(2)	1432(2)	41(1)
O(10)	5354(2)	7058(2)	3157(2)	36(1)
O(11)	5115(2)	8092(2)	1819(2)	38(1)
O(12)	8170(2)	6959(2)	2800(2)	40(1)
O(13)	5370(2)	8734(2)	3009(2)	37(1)
O(14)	5422(2)	5576(2)	3067(2)	39(1)
O(15)	8313(2)	7755(2)	3927(2)	53(1)
O(16)	7969(2)	6932(2)	184(2)	49(1)
N(1)	5468(3)	6310(2)	271(2)	47(2)
N(3)	3989(3)	7057(2)	1224(2)	44(2)
N(5)	4861(3)	8016(2)	269(2)	42(2)
N(7)	8918(3)	8901(3)	1629(3)	48(2)
N(9)	7391(3)	10057(2)	2073(2)	45(2)
N(11)	7557(3)	9271(2)	666(2)	45(2)
N(13)	9376(3)	5553(3)	2137(2)	48(2)
N(15)	8397(3)	5427(2)	3510(2)	47(2)
N(17)	7957(3)	4726(2)	2188(2)	46(2)
N(19)	5593(3)	7102(2)	4704(2)	41(2)
N(21)	5775(3)	8727(2)	4611(2)	42(2)
N(23)	4223(3)	8244(2)	4173(2)	41(2)

[a] Coordinates of the atoms outside the cluster core have been deposited. [b] Equivalent isotropic **U** defined as one-third of the trace of the orthogonalized $\mathbf{U}_{ij}$ tensor.

$4CH_3CN$ indicated partial disorder of the ring. The disordered pair share two common ring atoms; refinement of the disorder led to a site occupation of 0.80(1) for the dominant orientation. Positions of the subordinate ring atoms were initially refined and then fixed to ride on the dominant orientation during the last stages of refinement. Hydrogen atom positions were not calculated for the subordinate orientation, and fixed common isotropic thermal parameters were assigned for the remaining hydrogens. A thermal ellipsoid plot of the cluster core with atom labeling is presented in Figure 1. Selected bond lengths and angles for the cluster core are presented in Table 4.

The structure of the tetranuclear complex in compound **II** is similar to that in **I**·$4CH_3CN$. The refinement of **II** was hampered, however, by severe disorder problems and a shortage of high-angle data. Although the structural features of **II** are unambiguous, the agreement factors remain unacceptably high (>10%). Hence we do not report the full structure of **II**, noting instead its similarity to **I**·$4CH_3CN$ with the exception that the cocrystallized solvate molecules in **II** are toluene rather than acetonitrile.

Refinement of the structure of **IV** revealed clear disorder of the *tert*-butyl group attached to the N(31) pyrazole ring. Two orientations of the *tert*-butyl group were refined as rigid body groups free to rotate independently. Site occupation factors for the two orientations are 0.446(3) (unprimed atoms) and 0.555(3) (primed atoms). The four acetonitrile solvate molecules showed some instability in the refinement and were loosely constrained to a linear geometry with C−N and C−C bond lengths fixed at 1.135 and 1.438 Å, respectively. A relatively large but isolated difference map peak was also located and was interpreted as the oxygen atom of a partially included water of hydration. Least-squares refinement of this oxygen atom yielded a high degree of correlation between the thermal parameter and the site occupation factor.

Table 3. Atomic Coordinates ($\times 10^4$) and Equivalent Isotropic Displacement Coefficients ($Å^2 \times 10^3$) for $(t\text{-Bupz})_5V_4O_4(\mu\text{-}C_6H_5PO_3)_4\cdot 4CH_3CN\cdot 0.6\ H_2O$[a]

	x	*y*	*z*	U_{eq}[b]
V(1)	7015(2)	5399(1)	1373(1)	35(1)
V(2)	5652(2)	8233(1)	1085(1)	33(1)
V(3)	8838(2)	7013(2)	2100(1)	37(1)
V(4)	5530(2)	7066(2)	3112(1)	36(1)
P(1)	7687(3)	7065(2)	769(2)	35(1)
P(2)	6368(3)	8286(2)	2599(2)	33(1)
P(3)	7845(2)	5571(2)	2543(2)	35(1)
P(4)	4760(3)	6801(2)	1721(2)	35(1)
O(1)	5381(6)	6605(5)	3859(4)	45(2)
O(2)	9983(6)	6401(6)	1998(4)	48(2)
O(3)	6263(5)	7749(5)	3296(4)	37(2)
O(4)	5029(6)	9296(5)	991(4)	46(2)
O(5)	7390(5)	8066(5)	2285(4)	37(2)
O(6)	8334(6)	6165(5)	2633(4)	41(2)
O(7)	8158(5)	5096(5)	1840(4)	41(2)
O(8)	4840(5)	6686(5)	2518(4)	39(2)
O(9)	4660(5)	7742(5)	1412(4)	33(2)
O(10)	6743(5)	6078(5)	2617(4)	39(2)
O(11)	7009(5)	8096(5)	761(4)	33(2)
O(12)	8500(5)	6816(5)	1179(4)	31(2)
O(13)	7450(6)	4797(5)	693(4)	46(2)
O(14)	5607(5)	6028(5)	1296(4)	39(2)
O(15)	6972(6)	6627(5)	1044(4)	41(2)
O(16)	5788(5)	8082(5)	2119(4)	33(2)
N(11)	8989(7)	8202(7)	1593(5)	43(2
N(21)	8853(7)	7366(7)	3141(5)	39(2)
N(31)	5627(7)	7926(7)	44(5)	41(2)
N(41)	4211(7)	8280(7)	3265(6)	40(2)
N(51)	6724(7)	4420(6)	2070(5)	39(2)

[a] Coordinates of atoms outside the cluster core have been deposited. [b] Equivalent Isotropic **U** defined as one-third of the trace of the orthogonalized $\mathbf{U}_{ij}$ tensor.

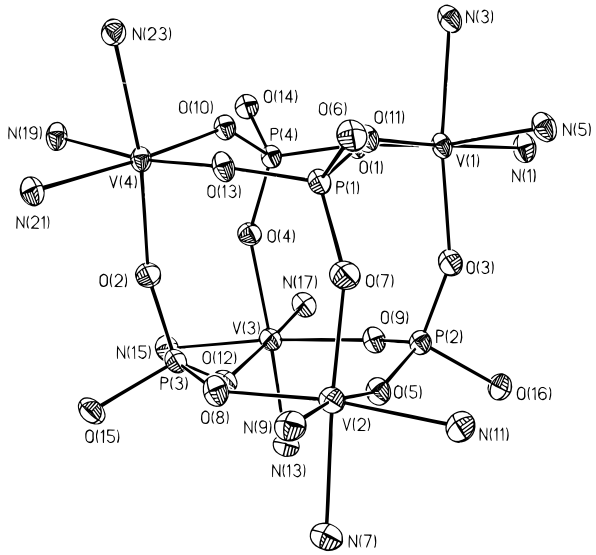

Figure 1. Thermal ellipsoid plot (20%) of the cluster core in **I**·$4CH_3$-CN with atom labels.

As a result the site occupation factor of the lattice water was fixed at 0.6 for the remainder of the refinement. A thermal ellipsoid plot of the cluster core of **IV** with atom labeling is shown in Figure 2. Selected bond lengths and angles for the cluster core are presented in Table 5.

Results

Structure of $[HB(pz)_3]_4V_4(\mu\text{-}C_6H_5OPO_3)_4\cdot 4CH_3CN$, I·$4CH_3CN$. The core geometry of this compound can be described as a cubane-type vanadium(III) phosphate cluster with octahedral vanadium and tetrahedral phosphorus centers located on alternate corners of the cube and oxygen atoms located

Table 4. Selected Bond Lengths (Å) and Bond Angles (deg) for $[HB(pz)_3]_4V_4(\mu\text{-}C_6H_5OPO_3)_4\cdot 4CH_3CN$, **I**·4CH$_3$CN[a]

V(1)−O(1)	1.966(3)	V(1)−N(5)	2.119(4)
V(1)−O(3)	1.956(3)	P(1)−O(6)[b]	1.613(3)
V(1)−O(11)	1.965(3)	P(1)−O(7)	1.494(4)
V(1)−N(1)	2.113(4)	P(1)−O(11)	1.500(4)
V(1)−N(3)	2.118(4)	P(1)−O(13)	1.509(3)
O(1)−V(1)−O(3)	95.7(1)	O(11)−V(1)−N(3)	93.2(1)
O(1)−V(1)−O(11)	93.5(1)	N(1)−V(1)−N(3)	84.9(2)
O(3)−V(1)−O(11)	93.9(1)	O(1)−V(1)−N(5)	171.4(2)
O(1)−V(1)−N(1)	92.8(1)	O(3)−V(1)−N(5)	92.6(1)
O(3)−V(1)−N(1)	87.6(2)	O(11)−V(1)−N(5)	88.2(1)
O(11)−V(1)−N(1)	173.4(1)	N(1)−V(1)−N(5)	85.3(2)
O(1)−V(1)−N(3)	88.4(2)	N(3)−V(1)−N(5)	83.1(2)
O(3)−V(1)−N(3)	171.6(2)		
$(O-P-O)_{mean}$[c]	113.6(8), 106.6(6), 101.9(7)		
$(V-O-P)_{mean}$[c]	153.6(22), 146.5(31), 138.8(5)		

[a] Estimated standard deviations in the least significant digit(s) are given in parentheses. [b] $(P-O)_{ester}$. [c] There are three sets of O−P−O and V−O−P bond angles; see text.

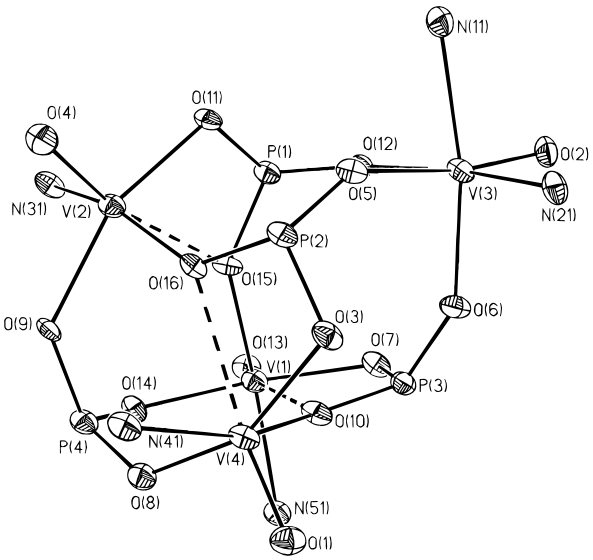

Figure 2. Thermal ellipsoid plot (20%) for the cluster core of **IV** with atom labels. Weak axial interactions in three vanadyl coordination octahedra are denoted by dashed lines.

midway along every edge of the cube. The compound employs the potentially tridentate monophenyl phosphate group, which can coordinate three different vanadium centers, as the bridging ligand while the vanadium centers, in turn, can be coordinated by three different phosphates.

In spite of the pleasingly simple structure of this tetranuclear cluster, it possesses no inherent crystallographic symmetry. Packing forces undoubtedly play a large role in the symmetry-reducing deformation of the cluster with the disposition of the peripheral groups taking the lead in symmetry reduction. The phenyl rings, in particular, are directed away from two opposite faces of the cube in an arrangement that would produce $\bar{4}$-symmetry at best. There is, in fact, an elongation of the core structure coincident with this phenyl ring orientation that suggests packing forces even influence the internal structure of the cluster. This elongation of the cubane core is shown by the four largest V−O−P angles which are found for the set of four edges, bisected by O(2), O(3), O(4), and O(7), that parallel the phenyl ring axes. Further consideration of the V−O−P angles reveals similar values among parallel sets. The set of four angles indicative of the elongation all have values greater than 150° (average = 153.6°), but there is also a set of four angles with values less than 140° (average = 138.8°) indicative

Table 5. Selected Bond Lengths (Å) and Bond Angles (deg) for $(t\text{-Bupz})_5V_4O_4(\mu\text{-}C_6H_5PO_3)_4\cdot 4CH_3CN\cdot 0.6\ H_2O$, **IV**[a]

V(1)−O(13)	1.578(9)	P(1)−O(12)	1.482(9)
V(1)−O(7)	1.970(9)	P(1)−O(15)	1.560(11)
V(1)−O(14)	1.989(8)	$(V=O)_{mean}$	1.579(13)
V(1)−O(15)	2.010(9)	$(V-N)_{mean}$[b]	2.119(11)
V(1)−N(51)	2.117(11)	$(V-N)_{mean}$[c]	2.148(18)
P(1)−O(11)	1.541(7)		
O(7)−V(1)−O(13)	103.5(4)	$(O-V-O)_{cis,mean}$[b]	88.0(5)
O(7)−V(1)−O(14)	154.0(4)	$(O=V-N)_{mean}$[b]	96.2(5)
O(13)−V(1)−O(14)	102.5(4)	$(O-V-N)_{trans,mean}$[b]	159.4(20)
O(7)−V(1)−O(15)	90.8(4)	$(O-V-N)_{cis,mean}$[b]	87.6(15)
O(13)−V(1)−O(15)	105.7(4)	O(2)═V(3)−O(5)	167.1(5)
O(14)−V(1)−O(15)	83.3(4)	$(O=V-O)_{cis,mean}$[c]	101.9(8)
O(7)−V(1)−N(51)	88.2(4)	$(O-V-O)_{cis,mean}$[c]	88.5(26)
O(13)−V(1)−N(51)	96.6(4)	$(O=V-N)_{mean}$[c]	92.0(9)
O(14)−V(1)−N(51)	87.7(4)	$(O-V-N)_{trans,mean}$[c]	165.9(18)
O(15)−V(1)−N(51)	157.2(4)	$(O-V-N)_{cis,mean}$[c]	83(5)
$(O=V-O)_{mean}$[b]	103.2(11)	N(11)−V(3)−N(21)	93.3(4)
$(O-V-O)_{trans,mean}$[b]	153.9(5)		
$(O-P-O)_{mean}$[d]	113.7(17), 103.8(13)		
$(V-O-P)_{mean}$[d]	139(6), 107.6(21), 85.3(18)		

[a] Estimated standard deviations in the last one or two significant digits are given in parentheses. Standard deviations in the last one or two digits about the mean are given in parentheses for average values. [b] Pertaining to V(1), V(2), and V(4). [c] Pertaining to V(3). [d] There are two sets of O−P−O and three sets of V−O−P bond angles; see text.

of a compression of the cubane core along a perpendicular direction. Finally, the remaining set of four angles takes on values between 140 and 150° (average = 146.5°) to give an overall rhombic distortion to the cluster core.

Local metal geometries are, in general, much more regular and consistent than the bridging geometry of the core. The vanadium centers all have (approximate) trigonally-distorted octahedral geometries with three sites of one octahedral face occupied by the nitrogen atoms of the terminal capping ligand ($[V-N]_{mean}$ and $[N-V-N]_{mean}$: 2.117(4) Å, 84.4(12)° for V(1); 2.107(6) Å, 84.2(11)° for V(2); 2.116(13) Å, 84.2(6)° for V(3); 2.105(4) Å, 84.3(14)° for V(4)) and the three sites of the opposite face occupied by oxygen atoms of three bridging mono(phenyl phosphate) groups ($[V-O]_{mean}$ and $[O-V-O]_{mean}$: 1.962(6) Å, 94.4(12)° for V(1); 1.959(7) Å, 94.4(10)° for V(2); 1.962(7) Å, 94.6(9)° for V(3); 1.970(3) Å, 94.1(15)° for V(4)).

Structure of $(t\text{-Bupz})_5V_4O_4(\mu\text{-}C_6H_5PO_3)_4\cdot 4CH_3CN\cdot 0.6H_2O$, IV. In contrast to the simple cubane-like geometry of **I** and **II**, the structure of **IV** might be better described as a trinuclear basket-shaped subcluster capped by a fourth vanadyl complex. The bottom of the basket is formed by a phosphonate group (P(4)) that simultaneously coordinates all three vanadyl centers of the subcluster. The three vanadyl centers of the basket are, in turn, each coordinated in the equatorial plane by a single pyrazole nitrogen and three phosphonate oxygen atoms. The sixth position, *trans* to the vanadyl oxygen, is occupied at all three metal centers by another phosphonate oxygen. This *trans* coordination is achieved through bidentate chelation of the vanadyl complex by one of the bridging phosphonates. In addition, the oxygen coordinated to the *trans* position of one vanadyl complex simultaneously coordinates the equatorial plane of a neighboring vanadyl complex. An isolated example of this bidentate chelate/bridging mode has been noted previously in a vanadyl phosphate cluster,[18] but this is a rare example where this mode is the dominant feature of the bridging framework. The *trans* V···O distances for V(2), 2.513 Å, and V(4), 2.474 Å, agree well with that previously observed, 2.475 Å.[18] The *trans* V···O distance observed for V(1), 2.615 Å, is significantly longer, however, and may indicate an interaction that is more

formal than real. Three bridging phosphonate groups, the three chelating phosphonates, are found to link the basket-like substructure to the fourth complex (V(3)). In this last complex, two of the equatorial sites are occupied by pyrazole nitrogen atoms and two by phosphonate oxygen atoms. The position *trans* to the vanadyl oxygen is occupied by a third phosphonate oxygen, but bidentate chelation is not found about this vanadium. In each of these complexes the vanadium centers V(1), V(2), V(4), and V(3) are raised above their basal planes by 0.42, 0.39, 0.39, and 0.25 Å, respectively. These deviations correlate well with increasing length (and presumably decreasing bond strength) of the atoms coordinated *trans* to the vanadyl oxygens.

Three of the O−P−O angles involving the PO_3 groups (one each from P(1), P(2), and P(3)) are approximately 104° whereas the remaining nine are greater than 110° (mean = 113.7(5)°). These differences may be explained in terms of the four-membered rings formed as a result of chelation by these phosphonate oxygens; i.e., the interior O−P−O angles of the rings are smaller (∼104°) than the exterior ones (∼114°). This explanation is supported by the fact that all the O−P−O angles involving the P(4) phosphonate group, which does not chelate, are greater than 110°. The same explanation applies to the observation of three sets of P−O−V angles with mean values of 85(2), 108(2), and 139(6)°, the first two sets corresponding to chelating oxygens in axial and equatorial sites, respectively, of the vanadyl octahedra.

Molecular Geometries of $[HB(pz)_3]_4V_4(\mu\text{-}C_6H_5OPO_3)_4$, I, $[HB(pz)_3]_4V_4(\mu\text{-}4\text{-}O_2NC_6H_4OPO_3)_4\cdot 4C_7H_8\cdot H_2O$, II, and ($t$-Bupz)$_4V_4O_4[\mu\text{-}C_6H_5PO_3)_4\cdot 2H_2O$, III. The loss of the acetonitrile molecules of solvation in **I**·4CH_3CN to give **I** is not expected to lead to any changes in the core structure since the solvent molecules are well-outside the cluster core. Indeed the structure of **II** as determined by X-ray crystallography shows the same core structure as found in **I**·4CH_3CN in spite of the differences in composition of the phosphate group and the included solvent. The similarity of the structures of **I** and **II** is also supported by the observed similarity in their spectral properties. For **III**, we propose the same core structure found in **IV** but with V(3) being coordinated by only one *tert*-butylpyrazole ligand rather than by two. This should result in a more symmetric structure for **III** with all the vanadium atoms having similar ligation.

Spectral, Electrochemical, and Magnetic Properties. The room temperature EPR spectrum of (t-Bupz)$_4V_4O_4(\mu$-C_6H_5-$PO_3)_4\cdot 2H_2O$, **III**, exhibits a single broad line ($g = 1.982$). The broad line, a characteristic of multispin systems, and g value confirm the occurrence of this compound as a polyvanadyl cluster. No EPR signal was observed for the vanadium(III) compounds $[HB(pz)_3]_4V_4(\mu\text{-}C_6H_5OPO_3)_4$, **I**, and $[HB(pz)_3]_4V_4(\mu$-4-$O_2NC_6H_4OPO_3)_4\cdot 4C_7H_8\cdot H_2O$, **II**. The visible and selected infrared spectral data are given in the Experimental Section.

The cyclic voltammogram of complex **I** was examined in CH_3CN and CH_2Cl_2. In acetonitrile two reversible oxidations of the cluster are observed at +0.68 and +1.13 V (vs Ag/AgCl). Extending the sweep range leads to additional poorly resolved oxidation processes that result in the degradation of the core structure as indicated by the loss of the return waves on the two initial oxidations. In CH_2Cl_2 the electrochemical behavior is similar, although there is a decrease in the reversibility of the oxidations as indicated by the increasing $P_a - P_c$ peak separation (75 mV in CH_3CN vs 225 mV in CH_2Cl_2). The additional electrochemical behavior beyond 1.2 V resolves into two further oxidations. Scanning through these processes also results in the loss of reversibility of the first two oxidations. In scrupulously clean and dry solvent, using freshly recrystallized supporting electrolyte, it is possible to scan through the four oxidations while retaining quasireversibility in the first three waves (see Figure 3). The four oxidations clearly correspond to the sequential one-electron oxidation of each vanadium(III) in the cluster to vanadium(IV). Substitution of the *p*-nitrophenyl phosphate for the simple phenyl phosphate pushes the redox potentials approximately 250 mV more positive, thereby making the cluster more difficult to oxidize, and only two waves are visible within the solvent window. While this is the expected trend for an electron-withdrawing substituent, it demonstrates that the peripheral phosphate ligation has a significant effect on the electronic nature of the vanadium centers. We had hoped to determine if the oxidations were localized over the entire cluster via controlled potential electrolysis and EPR. However, despite the quasireversibility on the cyclic voltammetry time scale, the oxidations on a bulk scale were irreversible, and hence no useful information was attainable in this regard.

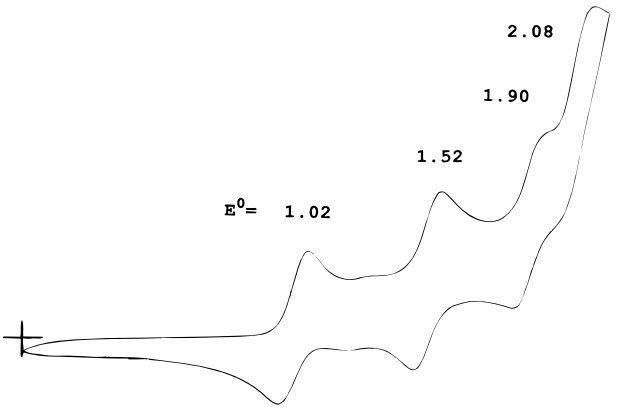

Figure 3. Cyclic voltammogram for compound **I**.

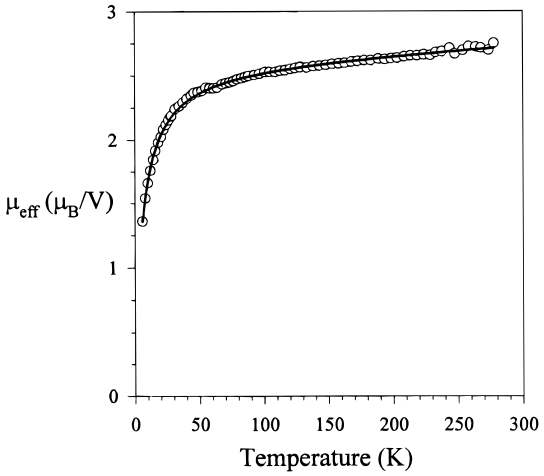

Figure 4. Plot of the effective moment per vanadium vs temperature for **I**·4CH_3CN (○, experimental; —, theoretical fit).

The effective magnetic moment per vanadium(III) ion in **I**·4CH_3CN is 2.60 μ_B at 278 K, decreases gradually to a value of 2.29 μ_B at 40 K, and then decreases more rapidly to 1.30 μ_B at 6 K as shown in Figure 4. These values indicate weak antiferromagnetic coupling in the system leading to a ground spin state with $S = 0$ and were modeled assuming uniform coupling between all spins of the cluster. The usual quadratic HDVV spin hamiltonian for the $S = 1$ cluster can be expressed more simply as

$$H = -J(S^2 - s_1^2 - s_2^2 - s_3^2 - s_4^2)$$

Diagonalization of this Hamiltonian yields three spin singlets

at $E = 8J$, six triplets at $E = 6J$, six quintets at $E = 2J$, three septets at $E = -4J$, and a nonet at $E = -12J$. Incorporating these energies and degeneracies into the van Vleck equation produces an expression for the product of susceptibility with temperature (χT) that fits the observed data very well (Figure 4). Best fit values using this theoretical model are as follows: $J/k = -2.64(4)$ K, $g = 1.827(5)$, and TIP = 0.00167(8) emu/mol.

A preliminary data set for compound **III** was measured, and a Curie−Weiss fit of the data yielded $\theta = -16.3$ K and $g = 1.98$.[27] This indicates moderately strong antiferromagnetic coupling within the cluster. Due to the uncertainty in the structural details of this cluster, however, an unambiguous model for the magnetic coupling could not be deduced. Consequently we have not pursued a more detailed analysis of the magnetic data for this compound. The difficulty in obtaining a pure bulk sample of **IV** has prevented measurement of its susceptibility.

Discussion

Synthesis. (*t*-Bupz)$_2$VOCl$_2$ and $C_6H_5PO_3Na_2 \cdot xH_2O$ react in water to give a blue precipitate which, upon recrystallization from ethanol, yields (*t*-Bupz)$_4$V$_4$O$_4$(μ-$C_6H_5PO_3$)$_4 \cdot 2H_2O$, **III**, as blue crystalline plates. Recrystallization of the same product from acetonitrile, on the other hand, gives a mixture of blue and purple products. The former has been shown by an X-ray structural study to be (*t*-Bupz)$_5$V$_4$O$_4$(μ-$C_6H_5PO_3$)$_4 \cdot 4CH_3CN$. This critical dependence of the composition and structure of compounds in the vanadium phosphate/phosphonate system on reaction conditions has been noted before.[5,8,11]

It is interesting to note that the reaction of (*t*-Bupz)$_2$VOCl$_2$ (or [(*t*-Bupz)$_4$VO(H_2O)]Cl$_2$) with $C_6H_5PO_3Na_2 \cdot xH_2O$ in water gives the tetranuclear species, (*t*-Bupz)$_5$V$_4$O$_4$(μ-$C_6H_5PO_3$)$_4 \cdot 4CH_3CN \cdot 0.6\ H_2O$, **IV**, whereas reaction with $C_6H_5OPO_3Na_2 \cdot 2H_2O$ produces the hexanuclear complex, $H_2O \subset$ [(*t*-Bupz)(μ-$C_6H_5OPO_3$)VO]$_6$(H_2O)$_2 \cdot 2CH_3CH_2OH$.[17] The former has two vanadium(IV) coordination environments with regard to the number of bound *t*-Bupz groups; one vanadium atom is coordinated by two *t*-Bupz groups, and the other three vanadium atoms are each coordinated by one *t*-Bupz group. The hexanuclear compound, on the other hand, has three sets of vanadium(IV) centers distinguished by the presence of two, one, and zero *t*-Bupz molecules. These results indicate that (*t*-Bupz)$_2$VOCl$_2$ and [(*t*-Bupz)$_4$VO(H_2O)]Cl$_2$ disintegrate in aqueous solution to give similar species (including free *t*-Bupz molecules) which, in the presence of $C_6H_5PO_3Na_2 \cdot xH_2O$ or $C_6H_5OPO_3Na_2 \cdot 2H_2O$, self-assemble spontaneously to give the observed products. Both $C_6H_5PO_3^{2-}$ and $C_6H_5OPO_3^{2-}$ groups function as tridentate bridging groups in these compounds, and the reason for the preferential formation of a tetranuclear compound in one case and a hexanuclear one in another may lie in the presence of the ester oxygen atom in $C_6H_5OPO_3^{2-}$. In addition to imparting some flexibility between the phenyl group and the phosphorus atom, this linkage places the phenyl group at a greater distance away from the cluster framework. This could facilitate the formation of a larger unit than is possible with $C_6H_5PO_3^{2-}$.

Magnetic Properties. The effective magnetic moment per vanadium(III) ion in [HB(pz)$_3$]$_4$V$_4$(μ-$C_6H_5OPO_3$)$_4 \cdot 4CH_3CN$, **I**$\cdot 4CH_3CN$, is reduced from the spin-only value of 2.8 μ_B. This, combined with the temperature dependence of the moment, is indicative of intramolecular magnetic coupling between the vanadium(III) ions. In view of the large separation (~5.1 Å) between vanadium ions in this compound, direct coupling should be negligible and a superexchange mechanism involving the phosphate bridges is the probable exchange pathway. (The ability of phosphate bridges to propagate magnetic exchange is well documented.[9,10]) Since the V(III) magnetic orbitals are in the t_{2g} block, superexchange coupling should occur through metal−ligand d−π overlap. This coupling mode is relatively ineffective through a metal−ligand single bond and would account for the weak coupling observed in **I**$\cdot 4CH_3CN$. The intermetal distances within **III** are probably substantially shorter than those in **I**$\cdot 4CH_3CN$ (the intermetal distances within the basket subunit of cluster **IV** are, in fact, almost an angstrom shorter (mean = 4.16(3) Å)) which might account for the larger magnetic interaction observed in the former.

The O═V(OPO)$_2$V═O Bridge. One of the most fundamental structural elements in vanadium phosphate clusters and extended solids is the O═V(OPO)$_2$V═O bridging unit. These units occur in a wide range of configurations, and conformations and we have suggested that the ability of this structural unit to adapt to various intramolecular forces plays a major role in the formation and stability of vanadyl phosphate systems. The species described in this work present a unique opportunity to extend these ideas to the relatively new class of cluster systems that do not contain templating reagents. We have already identified[18] four major classes of vanadium phosphate bridge configurations: *cis/cis-syn*, *cis/cis-anti*, *cis/trans*, and *trans/trans*. These terms refer to the mode of coordination of the two bridging oxygens in the equatorial planes of the respective metal centers: *cis/cis* configurations occurring with *cis* coordination of the bridging oxygens at both metal centers, *trans/trans* occurring with *trans* coordination at both metal centers, and *cis/trans* occurring with *cis* coordination at one metal center and *trans* coordination at the other. A further distinction, *syn* or *anti*, is made for the relative orientation of the vanadyl oxygens in the *cis/cis* coordination mode. The *cis/cis* configurations appear to be the most common with only a few examples of *cis/trans* and *trans/trans* configurations known previously. The *cis/trans* bridging configuration is, surprisingly, the predominant bridging mode in **IV**. One known occurrence of this bridging mode is in a template-centered hexanuclear cluster in which interaction between the template molecule and the bridging unit is minimal.[18] The conclusion then that this bridging mode is dictated more by cluster connectivity requirements than by template interactions is reinforced by the overwhelming presence of this mode in the empty cluster reported in this work.

The three remaining bridging units in **IV** that connect the basket-like subcluster to the capping complex provide more unusual bridging geometries. One of these bridges is a *cis/cis-syn* complex upon which a large twist distortion is applied. The parent untwisted bridge is expected to be almost planar since the vanadium and phosphorus atoms of the bridging ring lie close (within 0.09 Å) to a common plane. (Most bridging rings observed show a significant amount of folding, so the near planarity of the parent untwisted ring in this case is unusual as is the large twist distortion.) The two other bridging units coordinate V(3) in an axial position and thus fall outside the range of our formal classification system. Examples of axially coordinated phosphate bridges are rare (although we have noted one in a previous work[18]), but the two found here indicate the need to expand our classification of bridging units to include categories for axial coordination such as *cis/axial*, *trans/axial*, and *axial/axial*. The two *cis/axial* units observed here consist of quasiplanar parent rings also suffering a substantial twist distortion. Examples of all three types of bridging rings observed in **IV** are shown in Figure 5.

(27) O'Connor, C. J. Private communication, 1995.

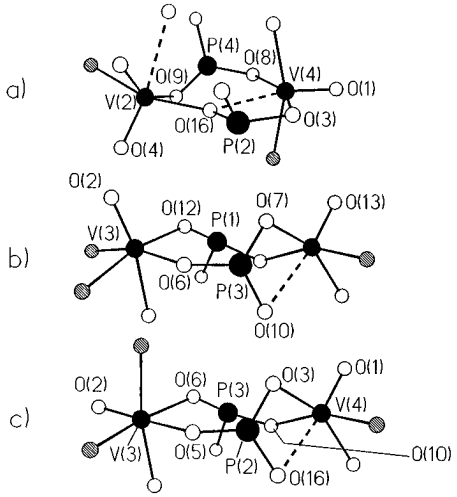

Figure 5. Ball-and-stick diagrams of the bridging $O{=}V(OPO)_2V{=}O$ units in the dimeric fragments of **IV**: (a) V(2)−V(4), a *cis*/*trans* bridge; (b) V(3)−V(1), a *cis*/*cis*-*syn* bridge; (c) V(3)−V(4), a *cis*/*axial* bridge. Weak V···O interactions are depicted by a dashed line. Vanadium atoms are small solid circles, oxygen atoms are small open circles, phosphorus atoms are large solid circles, and nitrogen atoms are small shaded circles. Labeled, terminal oxygen atoms are vanadyl oxygens.

Relationship to Template-Centered Clusters. The presence of template molecules or ions has been found to influence greatly the organization of vanadium phosphate clusters with the optimization of bonding of the host superstructure to the guest template playing a leading role in determining cluster structure.[2,5,6,18] Of particular interest with regard to the cluster compounds reported here are the fluoride-centered tetranuclear vanadium phosphonate clusters reported recently by Zubieta *et al.* [2] and Thorn *et al.*[28] These results indicate that the cavity of a tetranuclear cluster is large enough to accommodate the smallest template species, but in light of the compounds reported here, it must be concluded that a template molecule is not necessary for the formation of a closed cluster. However, the absence of the template guest molecule forces the vanadium complexes to complete their coordination spheres by other means. The presence of the tridentate capping ligand in compounds **I** and **II** gives coordinatively saturated vanadium complexes without resorting to a template guest molecule. The ensuing cubane-like structure achieves its regular geometry as a result of meeting cluster connectivity requirements. The effect of the absence of the template is more pronounced in compound **IV** in which the cluster forms with a collapsed structure so that bridging phosphate oxygen atoms can coordinate the axial sites, sites similar to those occupied instead by the fluoride template in the tetranuclear clusters reported in refs 2 and 28. Thus the closed clusters can form in the absence of a template molecule, but the structure is now determined by steric considerations and cluster connectivity requirements.

Acknowledgment. This work was supported by Robert A. Welch Foundation Grant AI-1157, Grant 3615-002 from the Texas Advanced Research Program, and National Institute of Health Grant GM4767601. NSF-ILI Program Grant USE-9151286 provided partial support of the X-ray diffraction facilities at Southwest Texas State University.

Supporting Information Available: Complete lists of atomic positions, complete listing of bond lengths and angles, anisotropic displacement parameters, hydrogen atom coordinates, data collection and crystal structure parameters, and stereoviews of the cluster frameworks for compounds $[HB(pz)_3]_4V_4(\mu\text{-}C_6H_5OPO_3)_4\cdot 4CH_3CN$ (**I**·$4CH_3CN$) and $(t\text{-Bupz})_5V_4O_4(\mu\text{-}C_6H_5PO_3)_4\cdot 4CH_3CN\cdot 0.6H_2O$ (**IV**) (28 pages). Ordering information is given on any current masthead page.

IC951017Z

(28) Thorn, D. L.; Harlow, R. L.; Herron, N. *Inorg. Chem.* **1995**, *34*, 2629.